Published in final edited form as:
Nanoscale. 2012 July 21; 4(14): 4073–4083. doi:10.1039/c2nr31192e.

Different Sized Luminescent Gold Nanoparticles

Jie Zheng, **Chen Zhou**, **Mengxiao Yu**, and **Jinbin Liu**
Department of Chemistry, University of Texas at Dallas, 800 W Campbell Rd, Richardson, TX, 75080, USA; Tel: +1-972-883-5768; Fax: +1-972-883-2925

Jie Zheng: jiezheng@utdallas.edu

Abstract

After one-decade's efforts, a large amount of highly luminescent metal nanoparticles with different sizes and surface chemistries have been developed. While the luminescence is often attributed to particle size effect, other structural parameters such as surface ligands, valence states of metal atoms and crystallinity of nanoparticles also have significant influence on emission properties and mechanisms. In this minireview, we summarized the strategies used to create luminescent gold nanoparticles with size from few to millions of atoms and discussed how these structural factors affect their photoluminescence.

I. Introduction

On the nanoscale, gold is a well-studied metal because of its tunable electronic structures and broad material properties.[1] Undoubtedly, surface plasmon absorption is the most fascinating property of gold nanoparticles (AuNPs), which fundamentally arises from collective oscillation of a large number of free electrons in a continuous band structure and can be tuned by changing many structural parameters such as particle size.[2] For example, for AuNPs with size larger than the wavelength of the light ($R>\lambda$), the frequency and bandwidth of surface plasmons can be quantitatively described with Mie theory.[1] When particle size approaches the electron mean free path (~50 nm for gold), decrease of particle size results in the blue shift of surface plasmons, which can still be described with a modified Mie theory.[1, 2] Other structural parameters such as shape, aggregation, composition and roughness also significantly influence surface plasmons and related properties such as surface enhanced Raman scattering (SERS), photothermal conversion.[3–6] Many excellent reviews help readers gain comprehensive understandings of these well-known plasmonic properties of AuNPs.[7–10]

In this review, we focus on luminescence property of AuNPs, which was much less well understood than surface plasmons. After one-decade's efforts, luminescent metal NPs start emerging as a new class of metal nanostructures.[11–14] New approaches for synthesis of different sized luminescent AuNPs with high quantum yields at large quantities have been developed, emission mechanisms have been partially unravelled, and a variety of applications of these AuNPs have been demonstrated. Since luminescent AuNPs with size ranging from 0.3 to 20 nm have been synthesized by tuning different structural parameters such as particle size, surface ligands, valence state and grain size, it becomes necessary to summarize how these factors influence luminescence properties and emission mechanisms, which might help develop and apply luminescent metal NPs in the future.

Correspondence to: Jie Zheng, jiezheng@utdallas.edu.

While luminescent AuNPs are only being intensively researched in the past decade, observation of luminescence from gold metal can be dated back as early as 1969.[15] Mooradia used a 488 nm laser to excite gold and copper films and observed photoluminescence at 564 and 620 nm respectively. Since gold or copper film has a continuous conduction (sp) band structure, the observed quantized transitions (luminescence) were not attributed to intraband (within sp band) but interband (d-sp) transitions. Shown in Scheme 1 is the first optical mechanism proposed to explain the photoluminescence from gold and other metal films, where the emission results from the recombination of electrons at the Fermi energy level with the holes in the upper-lying d band. While the observation of photoluminescence from metals, a system with extremely large density of states and a large number of free electrons, was quite unusual compared to conventional known fluorophores, limited attention was paid to this field in the first 20 years after this work was published. A part of reason was because the quantum yield (QY) was only 10^{-10},[15] too small for the detailed understandings and practical applications of emission from metals. In 1986, photoluminescence from metal films regained some attentions because a continuous emission background was constantly observed during the studies of SERS of metal films.[16] Boyd et al. found that luminescence from gold films was in the range of 400 to 653 nm, and emission maxima were dependent on the excitation wavelengths and also the film roughness. Surface roughness can enhance photoluminescence intensities up to 6 times because of a local-field effect. This study further suggests that the emission from gold films resulted from direct radiative recombination of electrons below the Fermi level with holes in the d bands.

Luminescence was not just observed from gold films but small gold nanostructures. In 1998, Wilcoxon et al. observed relatively intense blue emission at 440 nm from AuNPs with size smaller than 5 nm.[17] Those blue emitting AuNPs were created through KCN etching and the QY of emission was about 10^{-5}, 10^5 times higher than that of bulk gold metal (10^{-10}). However, what exact species giving the emission was not clear. In 2000, Mohamed et al. observed luminescence at 560 nm from gold nanorods with a QY a million times higher that of bulk gold metal.[18] Interestingly, the QY was found to increase quadratically with excitation powers while the wavelength maximum increased linearly with the length. Emissions from these small AuNPs or gold nanorods were also attributed to the electron and hole interband recombination process, which was further enhanced by surface plasmons.

While the increases in the luminescence QYs of gold nanostructure was attributed to local electrical-field enhancement effect in these studies described above, several additional reports on luminescence from very small AuNPs suggested that surface plasmons might not be indispensible for high QY emission from gold nanostructures. In 2000, Whetten and coworkers reported the near-infrared luminescence from 1.1 and 1.7 nm gold NCs with QY up to $(4.4\pm1.5) \times 10^{-5}$.[19] In 2001, Huang et al. observed fluorescence at 770 nm with a QY of 3×10^{-3} from 1.7 nm AuNPs[20] and Link et al. observed 770 nm emission from Au_{28} nanoclusters (note: corrected as Au_{25} in later works) with a QY of 2×10^{-3},[21] which are more than 10^7 times higher than those of gold films. Since these very small AuNPs start behaving like molecules and exhibit no surface plasmons, local-field enhancement effect was no longer involved in the observed high quantum-yield emission. Link et al. further proposed a hypothesis that emission from molecular Au clusters can arise from both intraband (sp-sp) in addition to the previous known interband (sp-d) transitions (Scheme 2).[21]

These studies with others[22, 23] done more than ten years ago set a foundation for today's research on luminescent AuNPs. In the past decade, a large number of highly luminescent AuNPs with size ranging from 0.3 to 20 nm (corresponding to the number of gold atoms from several to millions of atoms) have been synthesized,[24–35] and fundamental understandings of emission mechanisms have also been greatly advanced.[11, 36, 37] Herein,

we summarize the progress of this field by emphasizing the factors that influence luminescence properties and emission mechanisms. Since luminescence has been observed from both nonplasmoic and plasmonic AuNPs, luminescent NPs can be divided into molecular luminescent AuNPs and plasmonic ones. For molecular AuNPs, we can further divide them into two subclasses: few-atom Au nanoclusters (AuNCs) and few-nm AuNPs. Particle size, surface ligands, valence states and grain size all have significant influence on the luminescence properties of AuNPs (Scheme 3).

II. Few-atom luminescent AuNCs

Electronic structure of a single AuNP is dependent on its particle size.[1, 2] When particle size becomes comparable to electron Fermi wavelength of gold metal (0.5 nm),[38, 39] continuous band structure of the NPs breaks into discrete energy states; as a result, AuNPs behave like molecules.[40–42] On this extremely small size scale, AuNPs are often called as nanoclusters (NCs). AuNCs were found to be luminescent in gas matrices at low temperature back in 1987. Harbich and colleagues created luminescent Au_2 and Au_3 embedded in argon matrices.[43] While these studies clearly indicated size-dependent emission of AuNCs, the quantitative correlations of particle size with emission wavelength were not clear.

IIa. Dendrimer encapsulated luminescent AuNCs: particle size effect

Dendrimers are repetitively branched molecules with well-defined molecular weights and small cavities, which have been used to host and deliver drug molecules. Inspired by these unique characteristics of dendrimers, we used dendrimers as templates to encapsulate few-atom AuNCs.[24] Water-soluble and biocompatible poly(amidoamine) (PAMAM) dendrimer (G4-OH or G2-OH) were first used for this purpose. After gold ions were introduced into the solution of PAMAM, an equivalent of $NaBH_4$ was added into the solution and some reduced gold atoms aggregated within the dendrimers to form very small dendrimerencapsulated AuNCs. Once the large NPs were removed through centrifugation, luminescent AuNCs were obtained. Well-defined molecular weight of PAMAM allowed us to use electron spray ionization (ESI) mass spectrometry to determine cluster size. The first dendrimer encapsulated AuNCs we discovered in 2003 were Au_8 clusters, which give blue emission at 455 nm. The QY of this blue emitting Au_8 clusters is about 4×10^{-1}, 100 times higher than any known luminescent AuNPs by that time. To further understand size-dependent emission from AuNCs, we tuned molar ratios between dendrimer and gold ions as well as the amount of $NaBH_4$ used in the reactions, a class of AuNCs with different emission maxima ranging from UV and IR were obtained.[36] Using ESI mass spectrometry, we were able to identify the sizes of different emissive AuNCs. For example, emissions at 3.22, 2.72, 2.43, 1.65, and 1.41 eV correspond to Au_5, Au_8, Au_{13}, Au_{23} and Au_{31} respectively (Fig. 1A).[36] For the small AuNCs, the dependence of emission energy on the number of gold atoms, N, in each AuNC (Fig. 1B) can be quantitatively fit with a simple scaling relation of $E_{Fermi}/N^{1/3}$, in which E_{Fermi} is the Fermi energy of bulk gold (5.53 eV), similar to the scaling law observed from electronic absorptions of alkali metal NCs in gas matrices. These results indicate that electronic structure of dendrimer coated few-atom AuNCs is determined by the number of free electrons in Au nanoclusters, following a free-electron (Jellium) model.[44–46]

IIb. Luminescent AuNCs coated by other ligands

Size-dependent emission from dendrimer coated AuNCs implies that ligands have little influences on the electronic structure of these dendrimer encapsulated AuNCs.[36] Therefore, it should be feasible to create luminescent AuNCs with the same emission but different ligands. Indeed, in the past decade, a large number of luminescent AuNCs coated with a variety of ligands have been synthesized. For example, Duan et al. used an etching method

to create polyethylenimine (PEI) coated luminescent Au_8 clusters, which exhibited excitation and emission identical to dendrimer coated ones.[27] Muhammed et al. used glutathione to etch 4 nm mercaptosuccinic acid-protected AuNPs at pH 7~8 and obtained glutathione coated Au_8 clusters, which give the same blue emission as dendrimer coated ones do.[32] Zhou et al. were also able to create Au_8 clusters by etching AuNPs and nanorods with different biomolecules such as amino acids, peptides, proteins, and DNA,[47] further confirming that emission from few-atom AuNCs is solely dependent on their sizes and independent of surface ligands. While blue emitting Au_8 were one of the most common species synthesized at ambient conditions because of its close shell structure, other sized luminescent AuNCs coated with different ligands were also synthesized. For instance, Jin et al. observed UV emission at 340 nm from $Au_3(SC_{12}H_{25})_3$.[26] González et al. used poly(N-vinylpyrrolidone) (PVP) as a stabilizer to create Au_2 and Au_3 clusters with emission at 315 nm (3.94 eV) and 335 nm (3.70 eV) respectively.[48] Emission from these few-atom AuNCs perfectly fits with the free electron/jellium model.

For larger AuNCs, their emission energy is slightly deviated from the perfect free-electron model because of electron screening effect and a small harmonic distortion in the potential energy well. Emission from larger AuNCs is given by:[49]

$$\Delta E_{emission} = \frac{E_f}{N^{1/3}} \left[1 - U\left(l_e^2 - l_g^2 - \frac{n+2}{3} \right) \right]$$

where l_e and l_g are the angular momenta of the excited and ground states, respectively, n is the shell number; and U is the distortion parameter. The third term accounts for the shape change of the potential surface as a function of size. Emissions from many large AuNCs such as Au_{25} coated with glutathione,[21] Au_{25} coated with bovine serum albumin (BSA)[33] or pepsin[50] can be well fit with the modified free-electron model.

IIc. Emission mechanism of AuNCs

Luminescence observed from few-atom AuNCs follows the free-electron model, suggesting that emission fundamentally arises from intraband (sp-sp) band rather than interband (sp-d) band transitions. Scheme 4 shows the evolution of energy level spacing of sp band with the number of cluster size.[11] With the increase of the gold atom number, the energy level spacing becomes smaller and smaller and eventually becomes comparable to thermal energy (kT), resulting in disappearance of luminescence. Conventional local electrical field enhancement was not involved in the emission from few-atom AuNCs, in contrast to emission observed from large gold nanorods and bulk gold films. Luminescence lifetimes of these few-atom AuNCs are on the order of nanoseconds, indicating that ligand-metal charge transfer was not involved in the observed size-dependent emission of NCs. While surface ligands have little influences on the emission from those few-atom AuNCs, it should be noted that the same sized AuNCs with various surface ligands often emit at the same wavelength but can have different QYs. Therefore, selecting appropriate ligands for different application purposes should be considered.

IId. AuNCs with emission not following free-electron model: surface ligand effect

While free-electron model has been widely used to explain size-dependent emission from many luminescent AuNCs, some AuNCs exhibit emissions that cannot be easily interpreted with this model. For example, Negishi et al. synthesized a class of glutathione (SG) coated AuNCs including $Au_{10}(SG)_{10}$, $Au_{15}(SG)_{13}$, $Au_{18}(SG)_{14}$, $Au_{22}(SG)_{16}$, $Au_{22}(SG)_{17}$, $Au_{25}(SG)_{18}$, $Au_{29}(SG)_{20}$, $Au_{33}(SG)_{22}$, and $Au_{39}(SG)_{24}$ and found that emissions from these

clusters are much less sensitive to their cluster size than dendrimer coated ones.[25] For example, both $Au_{10}(SG)_{10}$ and $Au_{15}(SG)_{13}$ exhibited two-colour emission at 827 and 413/427 nm; $Au_{18}(SG)_{14}$ and $Au_{25}(SG)_{18}$ both emit at 827 nm, and $Au_{29}(SG)_{20}$, $Au_{33}(SG)_{22}$ and $Au_{39}(SG)_{24}$ all emit at 885 nm.[25] In addition, Au_{25} coated with glutathione synthesized through different methods were also found to give slightly different emissions. For instance, Pradeep et al. created $Au_{25}(SG)_{18}$ that gave two emission peaks at 500 nm and 700 nm respectively,[51] rather than 827 nm observed by Negishi. The emissions from these glutathione-coated AuNCs are less size-dependent than dendrimer encapsulated ones, suggesting that surface ligands influence emission from AuNCs and additional emission mechanism exists.

Unravelling crystal structure has shed some light on structure-emission relationships of these thiolated luminescent AuNCs with less size-dependent emission. Single-crystal X-ray crystallographic studies on Au_{25} NCs coated with phenylethanethiol ligands show that Au_{25} cluster is composed of a centered icosahedral Au_{13} core and an exterior shell made of 6 S-Au-S-Au-S staples.[52] Time-dependent density functional theory (TDDFT) calculations on the electronic structure of Au_{25} clusters show that the HOMO and the lowest three LUMOs are mainly composed of 6sp atomic orbitals of gold and a certain degree of the S(3p)[52]. The other higher HOMO orbitals are mainly constructed from the $5d_{10}$ atomic orbitals of gold and hence constitute the d-band. The calculated absorption transitions are consistent with the experimental observations. For instance, the first peak (HOMO-LUMO) at 1.8 eV observed in the absorption spectrum of Au_{25} clusters can be viewed as a sp-sp transition, corresponding to observed emission at 700 nm (1.77 eV) (Fig. 2A&B). Recent ultrafast spectroscopic studies on relaxation of higher excited states provide more insights on understanding of photoluminescence mechanism of Au_{25} clusters. Goodson et al. found that 500 nm emission fundamentally arises from the electron-hole recombination in Au_{13} core with little perturbation from surface ligands, but NIR emission at 700 nm originates from the recombination of holes in ground core state and electron decayed from core excited states to S-Au-S-Au-S semirings (Fig. 2C).[53] Interestingly, if we just assume that Au_{13} core behaves like an isolated cluster, the observed short-wavelength emission at 500 nm (2.48 eV) from Au_{13} core of Au_{25} clusters is very close to the 2.43 eV emission from dendrimer coated Au_{13}, further suggesting that surface thiolate ligands induce little changes in the core electronic structure, and also implying that Jellium model might still be valid in explaining the visible emission from the cores of AuNCs coated by thiolate ligands. Less size-dependent emission in NIR range likely arises from hybrid electronic states involved with S-Au-S-Au-S staples, where ligand-metal (S-Au) charge transfer is involved. Jin et al. recently found that charge state and surface ligands also have significant influence on NIR emission wavelength and QYs of Au_{25} clusters.[54] Clearly, more detailed photophysical studies are needed for eventually illustrating how surface ligands influence photoluminescence mechanisms of such systems.

III. Luminescent few-nanometer AuNPs (few-nm AuNPs)

Due to large density of states and extremely small electron Fermi wavelength (0.5 nm) of gold metal, luminescence of AuNCs is much more sensitive to the size than that of semiconductor quantum dots (exciton Bohr radius: ~10 nm).[55] For example, once the number of Au atoms in a AuNC reaches 55 atoms (1.2 nm in diameter), $Au_{55}(PPh_3)_{12}Cl_6$ no longer fluoresce.[56] Recently, Qian et al. reported that $Au_{333}(SR)_{79}$ clusters (2.2 nm) starts to give surface plasmons at 520 nm because energy level spacing in the cluster is so small that collective oscillation of free electrons can occur.[57] These studies suggest that quantized states can rapidly diminish with the increase of the particle size from few atoms to few nanometers; therefore, in theory, the few-nm NPs should no longer give fluorescence. However, in the past decade, a large number of luminescent few-nm AuNPs (1.5~3 nm)

have been synthesized.[34, 58–62] suggesting that additional emission mechanisms exist in AuNPs. In this section, we separate this class of few-nm luminescent AuNPs from those few-atom luminescent AuNCs. Based on their emission wavelengths, we divide them into NIR emitting few-nm AuNPs and visible emitting few-nm AuNPs.

IIIa. NIR emitting few-nm luminescent AuNPs: surface ligand effect

NIR emission was not just observed from few-atom AuNCs with size as small as $Au_{39}(SG)_{24}$ as we described in section IId.[25] In 2005, Wang et al. reported the observation of NIR emission ranging from 800 nm to 1.3 μm from few-nm AuNPs with size around 2 nm (Fig. 3).[34] They proposed that size-independent emission originates from localized core surface states with size-independent energetics. In their later work, they found that polarity of the thiolated ligands influence quantum efficiencies of NIR-emitting AuNPs, further indicating that emission fundamentally arises from the surface states of molecular AuNPs. Because similar NIR emission was also observed from few-atom thiolated AuNCs, it is highly likely that NIR emissions observed from few-nm IR emitting AuNPs also arise from the S-Au-S-Au-S shells rather than pure Au cores.

IIIb. Glutathione coated few-nm luminescent AuNPs (GS-AuNPs) with visible emission: valence state effect

Back in 2005, we discovered another approach to make few-nm luminescent AuNPs.[58] By taking advantage of reducing property of glutathione and unique dissociation process of glutathione(GS)-gold(I) polymers, we were able to create 1.7 nm orange emitting AuNPs (OGS-AuNPs) with a maximum at 565 nm (Fig. 4A&B) and 2.1 nm yellow emitting AuNPs (YGS-AuNPs) with a maximum at 545 nm (Fig. 4C&D).[59] QYs of these few-nm GS-AuNPs were measured to be $4.0(\pm0.4)\times10^{-2}$, one order larger than those NIR emitting AuNPs. Element analysis indicates that the ratio of Au and GS in orange emitting AuNPs is 22:10, which is larger than those of $Au_{25}(SR)_{18}$[39, 52, 63–65] and $Au_{38}(SR)_{24}$[66–69] but comparable to Authiol ratio of $Au_{144}(SR)_{60}$.[70]

Different from those nonluminescent few-nm AuNPs/luminescent AuNCs, [21, 39, 71] the luminescent GS-AuNPs contain a large amount of gold(I) atoms. X-ray photoelectron spectroscopic (XPS) studies on Au $4f_{2/7}$ binding energy (BE) of gold atoms in the luminescent few-nm GS-AuNPs show that nearly 49% and 45% of Au atoms in the OGS-AuNPs and yellow emitting AuNPs (YGS-AuNPs) are in the Au(I) oxidation state respectively,[59] which are significantly different from IR emitting AuNPs composed of Au(0) atoms.[34] Since gold(I) atoms fail to donate free electrons to the particles, no surface plasmon absorption was observed from these few-nm visible emitting GS-AuNPs. After further reducing these luminescent GS-AuNPs with $NaBH_4$, luminescence of the NPs vanished and very weak surface plasmon absorption of gold NPs started emerging even though very little change in particle size before and after adding $NaBH_4$ was observed. These observations further confirmed that luminescence from these few-nm AuNPs is strongly dependent on the valence states of gold atoms in the particles.[59]

IIIc. Visible emitting few-nm AuNPs coated by other ligands

Influence of gold valence states on the emission of visible emitting AuNPs was not just observed from glutathione coated ones, many ~2 nm luminescent AuNPs coated with other thiolate ligands have also been synthesized in the past few years.[59–62] For example, Huang et al. used several different alkanethiol ligands such as 2-mercaptoethanol, 6-mercaptohexanol, and 11-mercaptoundecanol to stabilize 2.9 nm luminescent AuNPs with emission ranging from 500 nm to 618 nm.[72] Guo et al. later used 11-mercaptodundecanoic acid as a protecting group to stabilize 2.7 nm luminescent AuNPs with emission at 615 nm.[73] Shang et al. developed a one-pot synthesis approach to create 1.8 nm d-peniciliamine

(DPA)[74] and 1.4 nm dihydrolipoic acid (DHLA) coated luminescent AuNPs[61] with emission at 610 nm and 684 nm, respectively. The common feature for this class of luminescent AuNPs is that surface ligands are all made of thiolate compounds and a large amount of Au(I) atoms exist in the NPs.

IIId. Photoluminescence mechanism of few-nm luminescent AuNPs

Compared to those few-atom luminescent AuNCs that follow jellium model, few-nm luminescent AuNPs exhibit different photophysical properties. First, both IR and visible emitting AuNPs exhibit very large Stokes shifts while few-atom dendrimer coated AuNCs only have ~50 nm Stokes shifts.[11, 21, 24, 30, 36, 47] Such large Stokes shifts were very similar to those of luminescent gold(I)-thiol complexes/polynuclear Au(I) clusters, where hybrid S–Au charge transfer states are involved in luminescence transitions.[75–78]

The luminescence lifetime studies unravelled very intriguing electronic structures of luminescent AuNPs. For NIR emitting AuNPs, only microsecond lifetimes were obtained regardless of the excitation wavelengths, suggesting that emission must be involved with Au-S hybrid states.[62] However, for visible emitting AuNPs, very unique excitation wavelength-dependent lifetimes were observed. Using OGS-AuNPs as an example,[59] we found that photoluminescence lifetimes of the particles are strongly dependent on the excitation wavelengths. At 420 nm excitation, these visible emitting AuNPs exhibited microsecond emission, suggesting that the observed emission obtained results from S-Au hybrid states (Fig. 5A). However, the emission lifetimes of visible emitting few-nm AuNPs significantly decreased to 2.8 ns (81%)/33 ns (19%) when the excitation wavelength was shifted to 530 nm(Fig. 5B), which is different from luminescent gold(I) complexes and NIR emitting AuNPs,[34,75–78] suggesting that S-Au charge-transfer states are no longer involved in emission at 530 nm excitation. The observation of a dramatic decrease in lifetimes of the same emission at different excitation wavelengths indicates that triplet and singlet excited states are degenerate in energy in the visible emitting AuNPs, consistent with the previously theoretically predicated degeneracies between singlet and triplet states in Au_{55} clusters.[79]

While the detailed emission mechanisms of these few-nm luminescent AuNPs are still not clear, we hypothesized optical mechanisms based on previous studies on electronic structures of polynuclear Au(I) clusters, IR emitting AuNCs and fully reduced Au(0) NPs (Scheme 5). For IR emitting AuNPs, their emission mechanism will be very similar to that of IR emitting AuNCs except that Au(0) core in IR-emitting AuNPs is too large to exhibit discrete energy states. Thiolate ligands can form hybrid states with sp orbitals of surface gold atoms Au(0), constructing HOMO of the NPs. The large Stokes shifts and microsecond lifetimes observed from IR-emitting luminescent AuNPs suggest that S-Au charge transfer is involved in the emission. The emission likely arises from the decay of excited electrons from higher energy states in sp band to hybrid electronic states of surface gold atoms and thiolated ligands. For visible emitting AuNPs, strong Au(I)-S bonds were formed, constructing hybrid electronic states different from those of IR emitting ones, and the energy levels of those hybrid states in visible emitting ones are likely lower than some states in d band because these hybrid Au(I)-S states will not be involved in the emission if the particles are excited at 530 nm. Consequently, the emissions of visible emitting AuNPs likely arise from sp to d band transitions.

IV. Plasmonic luminescent AuNPs

While tuning particle size and valence state of gold atoms allow us to create a variety of small luminescent AuNPs with different surface chemistries, one common limitation of these two strategies is that these molecular luminescent AuNPs exhibit no surface plasmons because of the limited number of free electrons. As a result, many applications based on

plasmonic property are lost while we gain luminescence property. On the other hand, as discussed in the introduction section, photoluminescence indeed was observed from gold films and plasmonic Au nanorods.[15–17] Most recently, the work done by Gaiduk et al. used a high energy pulsed laser to convert nonluminescent 20 nm AuNPs into emissive ones with a QY of ~ 1.4×10^{-6}.[80] However, limited by the preparation method, origin of emission was not clear. We recently used a grain size effect to develop a class of highly polycrystalline AuNPs, which not only exhibit strong surface plasmons but also bright single-particle luminescence.[81]

IVa. Grain size effect in plasmonic luminescent AuNPs

Grain size effects have been widely observed from polycrystalline metallic thin films composed of grains with different sizes and orientations.[82–85] For example, due to grain-boundary scattering effects, a decrease in grain size often improves yield strength and hardness of materials[86–88] but reduces their electrical and thermal conductivities.[89, 90] While single-crystal gold films generally have very small enhancements on the Raman scattering of organic molecules on their surfaces, the increase of surface roughness by decreasing grain size can dramatically enhance Raman-scattering cross sections of organic molecules on the gold surface[91]. Not only Raman scattering, other linear or nonlinear optical properties of metallic films, such as absorption, fluorescence as well as two-photon emission, also change accordingly with crystallinity and grain size.[16] These fascinating changes in material properties of metal films fundamentally arise from the increase of grain boundaries and emergence of quantum confinement effects.

Plasmonic metal NPs (20~50 nm) also exhibit polycrystalline structure; therefore, grain size should also have significant influences on material properties of metal NPs, however, grain size effect in plasmonic metal NPs is much less understood because of lack of chemical synthesis of control of grain sizes. We recently developed a solid-state synthesis method that allows us to partially control grain sizes of the NPs.[81]

Luminescent plasmonic AuNPs of 20 nm were synthesized in solid-state through thermal reduction of gold-glycine complex at 453 K. High-resolution transmission electron microscopy (HR-TEM) studies showed that these AuNPs exhibit highly polycrystalline structures with grain size down to 1 nm (called as polycrystalline gold nanoparticles, pAuNPs, Fig. 6A) while commercially available ~20 nm AuNPs synthesized in liquid phase exhibit multi-twinned structure with grains of 8 nm (called as multi-twinned gold NP, mAuNP, Fig. 6B). The grain size distributions in the NPs were further quantified by investigating $4f_{7/2}$ electron binding energy (BE) of Au atoms in the NPs with XPS because the core-electron BE shift of a metal atom is inversely proportional to the grain size of metallic thin films.[92] Fig. 6C shows that Au $4f_{7/2}$ BE of commercially available ~20 nm mAuNPs exhibits a single Gaussian peak at 83.9 eV, which is blue shifted 0.2 eV compared to bulk gold metal (83.7 eV),[93] while two peaks at 84.0 eV and 85.1 eV were observed from ~20 nm pAuNPs. The additional peak at 85.1 eV was comparable to BE (85.1 eV) of Au_{55} clusters (1.2 nm).[94] Two BE shifts of 0.3 and 1.4 eV correspond to two different, 5 nm and 1 nm, grain-size populations in ~20 nm pAuNPs respectively, consistent with the observed highly polycrystalline structures of pAuNPs from TEM studies.

IVb. Emission mechanism of plasmonic luminescent AuNPs

pAuNPs not only exhibit strong surface plasmon absorption but also bright and robust single-particle luminescence.[81] Shown in Figure 7A is the absorption maximum of ~20 nm as-synthesized pAuNPs, which is red shifted about 16 nm compared to that of mAuNPs (520 nm). In addition, by fitting the absorption spectra of AuNPs with Lorentzian function, we found that the surface plasmon bandwidth, a characteristic of collision efficiency between

free electrons and surface atoms, of pAuNPs (105 nm) is much broader than that (81 nm) of the same sized mAuNPs but comparable to that (107 nm) of 5 nm AuNPs, indicating that the dephasing of coherent oscillations of free electrons (surface plasmons) in pAuNPs was greatly enhanced by the increase of grain boundaries.[95, 96]

Different from conventional plasmonic AuNPs that are often not luminescent due to extremely high density of states, pAuNPs exhibit strong luminescence at the single particle level (Fig. 7B). The average emission intensity of individual pAuNPs is comparable to that of individual commercially available semiconductor quantum dots under the same mercury lamp excitation conditions, suggesting that the emission cross section of pAuNPs is about 10^{-15} cm^2. Since surface plasmon absorption cross section of ~20 nm AuNPs is on the order of 10^{-13} cm^2,[97, 98] the estimated QY of pAuNPs is about 10^{-2} under such excitation conditions. While luminescence QY of pAuNPs is much smaller than those of few-nm luminescent AuNPs because of strong surface plasmon absorption,[11] luminescence brightness and stability of pAuNPs at the single particle level are one order and three orders higher than those of few-nm luminescent AuNPs respectively (Fig. 7C).[59, 99, 100]

The lifetime measurements indicated that the luminescence lifetimes of pAuNPs is less than instrumental response function (~35 ps) of ultrafast laser system, which is more than two-order shorter than those of few-nm luminescent AuNPs.[59, 99, 100] The increase in luminescence intensity and stability and the decrease of lifetime are consistent with previous observations that fluorescence intensities of quantum dots and other fluorophores near a rough gold surface can be increased about one order by surface plasmons,[101–105] implying strong coupling between surface plasmons of large grains and single-electron excitations of small grains within a single particle. Based on these studies, we hypothesized that continuous electron band and discrete energy states co-exist within one single particle (Fig. 7D). Under the light excitation, both surface plasmon absorption and single-electron transitions were excited, as a result, coupling between surface plasmons and luminescence become available, giving bright plasmon enhanced luminescence.

V. Summary and outlook

A large number of highly luminescent AuNPs with different sizes and versatile surface chemistries have been synthesized in the past decade. Emission can be tuned through changing particle size, surface ligands, valence states of Au atoms and grain size/boundary. While we have made significant progress on the understandings of emission mechanisms, most of these mechanisms are not completely clear. Therefore, deeper photophysical studies (lifetimes, Stokes shifts, transient absorption) and detailed structural characterizations (particle size, crystal structure, valence states, surface structure) will help us further unravel the origin of photoluminescence. The future of luminescent AuNPs will also heavily rely on their applications in targeting challenges that many other fluorophores hardly address. Chemical sensing and bioimaging applications of luminescent AuNPs have started to be demonstrated.[29–31, 72, 99, 100, 106–112] While we focus on luminescent AuNPs in this review, a large amount of luminescent silver, copper, platinum NPs have also been created using the similar synthetic strategies and follow similar emission mechanisms.[113–121] Considering unique densities of states, tunable electronic structures, diverse material properties and desired biocompatibilities of metal NPs, luminescent metal NPs will have a glowing future.

Acknowledgments

This work was supported in part by NIH (R21EB009853 and 1R21EB011762), CPRIT (120588) and the start-up fund from the University of Texas at Dallas.

References

1. Kreibig, U.; Vollmer, M. Optical Properties of Metal Clusters. Springer; 1995.
2. Ashcroft, NW.; Mermin, ND. Solid State Physics. HOLT, Rinehart and Winston; New York: 1976.
3. Jain PK, Huang XH, El-Sayed IH, El-Sayed MA. Acc Chem Res. 2008; 41:1578. [PubMed: 18447366]
4. Scher EC, Manna L, Alivisatos AP. Philos T Roy Soc A. 2003; 361:241.
5. Sun YG, Xia YN. Science. 2002; 298:2176. [PubMed: 12481134]
6. Caruso F, Caruso RA, Mohwald H. Science. 1998; 282:1111. [PubMed: 9804547]
7. Hu M, Chen JY, Li ZY, Au L, Hartland GV, Li XD, Marquez M, Xia YN. Chem Soc Rev. 2006; 35:1084. [PubMed: 17057837]
8. Huang XH, Jain PK, El-Sayed IH, El-Sayed MA. Nanomedicine-Uk. 2007; 2:681.
9. Jain PK, Huang X, El-Sayed IH, El-Sayad MA. Plasmonics. 2007; 2:107.
10. Grzelczak M, Perez-Juste J, Mulvaney P, Liz-Marzan LM. Chem Soc Rev. 2008; 37:1783. [PubMed: 18762828]
11. Zheng J, Nicovich PR, Dickson RM. Ann Rev Phys Chem. 2007; 58:409. [PubMed: 17105412]
12. Shang L, Dong S, Nienhaus GU. Nano Today. 2011; 6:401.
13. Diez I, Ras RHA. Nanoscale. 2011; 3:1963. [PubMed: 21409225]
14. Lin CAJ, Lee CH, Hsieh JT, Wang HH, Li JK, Shen JL, Chan WH, Yeh HI, Chang WH. J Med Bio Eng. 2009; 29:276.
15. Mooradia A. Phys Rev Lett. 1969; 22:185.
16. Boyd GT, Yu ZH, Shen YR. Phy Rev B. 1986; 33:7923.
17. Wilcoxon JP, Martin JE, Parsapour F, Wiedenman B, Kelley DF. J Chem Phys. 1998; 108:9137.
18. Mohamed MB, Volkov V, Link S, El-Sayed MA. Chem Phys Lett. 2000; 317:517.
19. Bigioni TP, Whetten RL, Dag O. J Phys Chem B. 2000; 104:6983.
20. Huang T, Murray RW. J Phys Chem B. 2001; 105:12498.
21. Link S, Beeby A, FitzGerald S, El-Sayed MA, Schaaff TG, Whetten RL. J Phys Chem B. 2002; 106:3410.
22. Apell P, Monreal R, Lundqvist S. Physica Scripta. 1988; 38:174.
23. Stuckless JT, Moskovits M. Phys Rev B. 1989; 40:9997.
24. Zheng J, Petty JT, Dickson RM. J Am Chem Soc. 2003; 125:7780. [PubMed: 12822978]
25. Negishi Y, Takasugi Y, Sato S, Yao H, Kimura K, Tsukuda T. J Am Chem Soc. 2004; 126:6518. [PubMed: 15161256]
26. Jin RC, Egusa S, Scherer NF. J Am Chem Soc. 2004; 126:9900. [PubMed: 15303846]
27. Duan H, Nie S. J Am Chem Soc. 2007; 129:2412. [PubMed: 17295485]
28. Eichelbaum M, Rademann K, Hoell A, Tatchev DM, Weigel W, Stoesser R, Pacchioni G. Nanotechnology. 2008:19.
29. Chen W, Tu X, Guo X. Chem Commun. 2009:1736.
30. Lin CAJ, Yang TY, Lee CH, Huang SH, Sperling RA, Zanella M, Li JK, Shen JL, Wang HH, Yeh HI, Parak WJ, Chang WH. ACS Nano. 2009; 3:395. [PubMed: 19236077]
31. Muhammed MAH, Verma PK, Pal SK, Kumar RCA, Paul S, Omkumar RV, Pradeep T. Chem-Eur J. 2009; 15:10110. [PubMed: 19711391]
32. Muhammed MAH, Verma PK, Pal SK, Retnakumari A, Koyakutty M, Nair S, Pradeep T. Chemistry-Eur J. 2010; 16:10103.
33. Xie J, Zheng Y, Ying JY. J Am Chem Soc. 2009; 131:888. [PubMed: 19123810]
34. Wang GL, Huang T, Murray RW, Menard L, Nuzzo RG. J Am Chem Soc. 2005; 127:812. [PubMed: 15656600]
35. Wu Z, Jin R. Nano Lett. 2010; 10:2568. [PubMed: 20550101]
36. Zheng J, Zhang CW, Dickson RM. Phys Rev Lett. 2004:93.
37. Jin R. Nanoscale. 2010; 2:343. [PubMed: 20644816]
38. Kubo R. J Phys Soc Jpn. 1962; 17:975.

39. Schaaff TG, Knight G, Shafigullin MN, Borkman RF, Whetten RL. J Phys Chem B. 1998; 102:10643.
40. Sanchez A, Abbet S, Heiz U, Schneider WD, Hakkinen H, Barnett RN, Landman U. J Phys Chem A. 1999; 103:9573.
41. Wallace WT, Whetten RL. J Am Chem Soc. 2002; 124:7499. [PubMed: 12071759]
42. Campbell CT, Parker SC, Starr DE. Science. 2002; 298:811. [PubMed: 12399586]
43. Fedrigo S, Harbich W, Buttet J. J Chem Phys. 1993; 99:5712.
44. Knight WD, Clemenger K, Deheer WA, Saunders WA, Chou MY, Cohen ML. Phys Rev Lett. 1984; 52:2141.
45. Deheer WA, Selby K, Kresin V, Masui J, Vollmer M, Chatelain A, Knight WD. Phys Rev Lett. 1987; 59:1805. [PubMed: 10035336]
46. Deheer WA. Rev Mod Phys. 1993; 65:611.
47. Zhou RJ, Shi MM, Chen XQ, Wang M, Chen HZ. Chemistry- Eur J. 2009; 15:4944.
48. Gonzalez BS, Rodriguez MJ, Blanco C, Rivas J, Lopez-Quintela MA, Martinho JMG. Nano Lett. 2010; 10:4217. [PubMed: 20836542]
49. Clemenger K. Phys Rev B. 1985; 32:1359.
50. Kawasaki H, Hamaguchi K, Osaka I, Arakawa R. Adv Funct Mater. 2011; 21:3508.
51. Shibu ES, Muhammed MAH, Tsukuda T, Pradeep T. J Phys Chem C. 2008; 112:12168.
52. Zhu M, Aikens CM, Hollander FJ, Schatz GC, Jin R. J Am Chem Soc. 2008; 130:5883. [PubMed: 18407639]
53. Devadas MS, Kim J, Sinn E, Lee D, Goodson T, Ramakrishna G. J Phys Chem C. 2010; 114:22417.
54. Qian HF, Sfeir MY, Jin RC. J Phys Chem C. 2010; 114:19935.
55. Alivisatos AP. Science. 1996; 271:933.
56. Schmid G, Liu YP. Nano Lett. 2001; 1:405.
57. Qian HF, Zhu Y, Jin RC. P Natl Acad Sci USA. 2012; 109:696.
58. Zheng, J. Fluorescent Noble Metal Nanoclusters Thesis (Ph D). Georgia Institute of Technology; Atanta: 2005.
59. Zhou C, Sun C, Yu MX, Qin YP, Wang JG, Kim M, Zheng J. J Phys Chem C. 2010; 114:7727.
60. Tang Z, Robinson DA, Bokossa N, Xu B, Wang S, Wang G. J Am Chem Soc. 2011; 133:16037. [PubMed: 21919537]
61. Shang L, Azadfar N, Stockmar F, Send W, Trouillet V, Bruns M, Gerthsen D, Nienhaus GU. Small. 2011; 7:2614. [PubMed: 21809441]
62. Tu X, Chen W, Guo X. Nanotechnology. 2011:22.
63. Dass A, Dubay GR, Fields-Zinna CA, Murray RW. Anal Chem. 2008; 80:6845. [PubMed: 18707129]
64. Akola J, Walter M, Whetten RL, Hakkinen H, Gronbeck H. J Am Chem Soc. 2008; 130:3756. [PubMed: 18321117]
65. Jiang DE, Dai S. Inorg Chem. 2009; 48:2720. [PubMed: 19236016]
66. Schaaff TG, Shafigullin MN, Khoury JT, Vezmar I, Whetten RL, Cullen WG, First PN, GutierrezWing C, Ascensio J, JoseYacaman MJ. J Phys Chem B. 1997; 101:7885.
67. Antonello S, Holm AH, Instuli E, Maran F. J Am Chem Soc. 2007; 129:9836. [PubMed: 17658798]
68. Pei Y, Gao Y, Zeng XC. J Am Chem Soc. 2008; 130:7830. [PubMed: 18517203]
69. Chaki NK, Negishi Y, Tsunoyama H, Shichibu Y, Tsukuda T. J Am Chem Soc. 2008; 130:8608. [PubMed: 18547044]
70. Lopez-Acevedo O, Akola J, Whetten RL, Gronbeck H, Hakkinen H. Abstr Pap Am Chem Soc. 2009:238.
71. Wu ZW, Gayathri C, Gil RR, Jin RC. J Am Chem Soc. 2009; 131:6535. [PubMed: 19379012]
72. Huang CC, Yang Z, Lee KH, Chang HT. Angew Chem Int Ed. 2007; 46:6824.
73. Guo YM, Wang Z, Shao HW, Jiang XY. Analyst. 2012; 137:301. [PubMed: 22048157]

74. Shang L, Dorlich RM, Brandholt S, Schneider R, Trouillet V, Bruns M, Gerthsen D, Nienhaus GU. Nanoscale. 2011; 3:2009. [PubMed: 21311796]
75. Vickery JC, Olmstead MM, Fung EY, Balch AL. Angew Chem Int Ed. 1997; 36:1179.
76. Yam VWW, Lo KKW. Chem Soc Rev. 1999; 28:323.
77. White-Morris RL, Olmstead MM, Jiang FL, Tinti DS, Balch AL. J Am Chem Soc. 2002; 124:2327. [PubMed: 11878988]
78. Lee YA, Eisenberg R. J Am Chem Soc. 2003; 125:7778. [PubMed: 12822977]
79. Magyar RJ, Mujica V, Marquez M, Gonzalez C. Phys Rev B. 2007:75.
80. Gaiduk A, Ruijgrok PV, Yorulmaz M, Orrit M. Phys Chem Chem Phys. 2011; 13:149. [PubMed: 21042602]
81. Zhou C, Yu J, Qin Y, Zheng J. Nanoscale. 201210.1039/C2NR30212H
82. Kobrinsky MJ, Thompson CV. Acta Materialia. 2000; 48:625.
83. Chae BG, Yang YS, Lee SH, Jang MS, Lee SJ, Kim SH, Baek WS, Kwon SC. Thin Solid Films. 2002; 410:107.
84. Zhang W, Brongersma SH, Clarysse T, Terzieva V, Rosseel E, Vandervorst W, Maex K. J Vac Sci Techol B. 2004; 22:1830.
85. Camacho JM, Oliva AI. Thin Solid Films. 2006; 515:1881.
86. Jin S, Hwang SK, Morris JW. Metall Trans A. 1975; 6:1721.
87. Lasalmonie A, Strudel JL. J Mater Sci. 1986; 21:1837.
88. Feaugas X, Haddou H. Philos Mag. 2007; 87:989.
89. Durkan C, Welland ME. Phys Rev B. 2000; 61:14215.
90. Karim S, Ensinger W, Cornelius TW, Neumann R. Physica E. 2008; 40:3173.
91. Moskovits M. J Chem Phys. 1978; 69:4159.
92. Wertheim GK, Dicenzo SB. Phys Rev B. 1988; 37:844.
93. Fuggle JC, Kallne E, Watson LM, Fabian DJ. Phys Rev B. 1977; 16:750.
94. Turner M, Golovko VB, Vaughan OPH, Abdulkin P, Berenguer-Murcia A, Tikhov MS, Johnson BFG, Lambert RM. Nature. 2008; 454:981. [PubMed: 18719586]
95. Hostetler JL, Smith AN, Czajkowsky DM, Norris PM. Appl Optics. 1999; 38:3614.
96. Canchal-Arias D, Dawson P. Surf Sci. 2005; 577:95.
97. Jain PK, Lee KS, El-Sayed IH, El-Sayed MA. J Phys Chem B. 2006; 110:7238. [PubMed: 16599493]
98. Liu XO, Atwater M, Wang JH, Huo Q. Colloids Surf B. 2007; 58:3.
99. Zhou C, Long M, Qin YP, Sun XK, Zheng J. Angew Chem Int Ed. 2011; 50:3168.
100. Yu M, Zhou C, Liu J, Hankins JD, Zheng J. J Am Chem Soc. 2011; 133:11014. [PubMed: 21714577]
101. Shimizu KT, Woo WK, Fisher BR, Eisler HJ, Bawendi MG. Phys Rev Lett. 2002:89.
102. Anger P, Bharadwaj P, Novotny L. Phys Rev Lett. 2006:96.
103. Pompa PP, Martiradonna L, Della Torre A, Della Sala F, Manna L, De Vittorio M, Calabi F, Cingolani R, Rinaldi R. Nat Nanotechnol. 2006; 1:126. [PubMed: 18654164]
104. Chen Y, Munechika K, Ginger DS. Nano Lett. 2007; 7:690. [PubMed: 17315937]
105. Zhang JT, Tang Y, Lee K, Ouyang M. Nature. 2010; 466:91. [PubMed: 20596017]
106. Wu X, He XX, Wang KM, Xie C, Zhou B, Qing ZH. Nanoscale. 2010; 2:2244. [PubMed: 20835443]
107. Wei H, Wang ZD, Yang LM, Tian SL, Hou CJ, Lu Y. Analyst. 2010; 135:1406. [PubMed: 20411205]
108. Xie JP, Zheng YG, Ying JY. Chem Commun. 2010; 46:961.
109. Pu KY, Luo ZT, Li K, Xie JP, Liu B. J Phys Chem C. 2011; 115:13069.
110. Liu CL, Wu HT, Hsiao YH, Lai CW, Shih CW, Peng YK, Tang KC, Chang HW, Chien YC, Hsiao JK, Cheng JT, Chou PT. Angew Chem Int Ed. 2011; 50:7056.
111. Yuan ZQ, Peng MH, He Y, Yeung ES. Chem Commun. 2011; 47:11981.

112. Sun CJ, Yang H, Yuan Y, Tian X, Wang LM, Guo Y, Xu L, Lei JL, Gao N, Anderson GJ, Liang XJ, Chen CY, Zhao YL, Nie GJ. J Am Chem Soc. 2011; 133:8617. [PubMed: 21542609]
113. Zheng J, Dickson RM. J Am Chem Soc. 2002; 124:13982. [PubMed: 12440882]
114. Petty JT, Zheng J, Hud NV, Dickson RM. J Am Chem Soc. 2004; 126:5207. [PubMed: 15099104]
115. Zheng J, Ding Y, Tian BZ, Wang ZL, Zhuang XW. J Am Chem Soc. 2008; 130:10472. [PubMed: 18636722]
116. Petty JT, Fan CY, Story SP, Sengupta B, Iyer AS, Prudowsky Z, Dickson RM. J Phys Chem Lett. 2010; 1:2524. [PubMed: 21116486]
117. Petty JT, Fan CY, Story SP, Sengupta B, Sartin M, Hsiang JC, Perry JW, Dickson RM. J Phys Chem B. 2011; 115:7996. [PubMed: 21568292]
118. Fan CY, Hsiang JC, Jablonski AE, Dickson RM. Chem Sci. 2011; 2:1080. [PubMed: 22262992]
119. Yuan X, Luo ZT, Zhang QB, Zhang XH, Zheng YG, Lee JY, Xie JP. ACS Nano. 2011; 5:8800. [PubMed: 22010797]
120. Wei WT, Lu YZ, Chen W, Chen SW. J Am Chem Soc. 2011; 133:2060. [PubMed: 21280578]
121. Choi S, Dickson RM, Yu JH. Chem Soc Rev. 2012; 41:1867. [PubMed: 22076614]

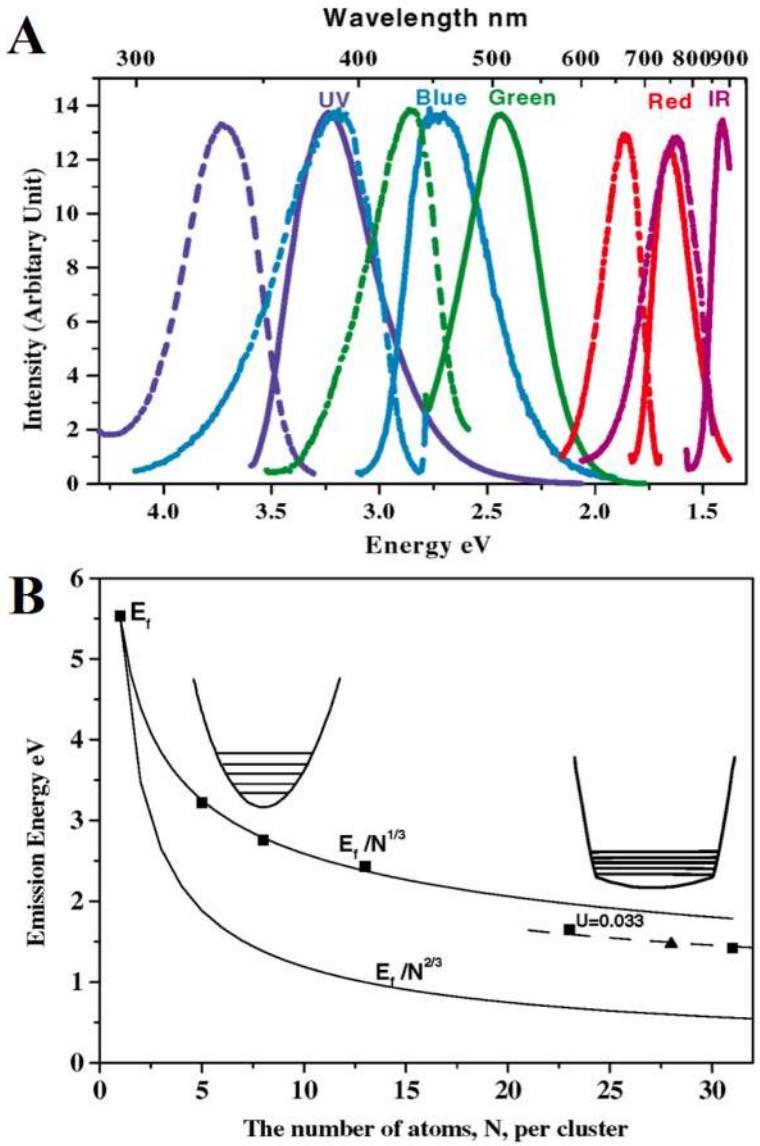

Figure 1.

(A) Excitation (dashed) and emission (solid) spectra of different gold nanoclusters. Excitation and emission maxima shift to longer wavelength with the increase of cluster size, suggesting that particle size governs emission from these few-atom gold nanoclusters; (B) Correlation of the number of gold atoms, N, per cluster with emission energy. Emission energy decreases with increasing number of atoms. The correlation of emission energy with N is quantitatively fit with $E_{Fermi}=N^{1/3}$, as predicted by the spherical jellium model. (Reprinted from Ref. 36, with permission from American Physical Society.)

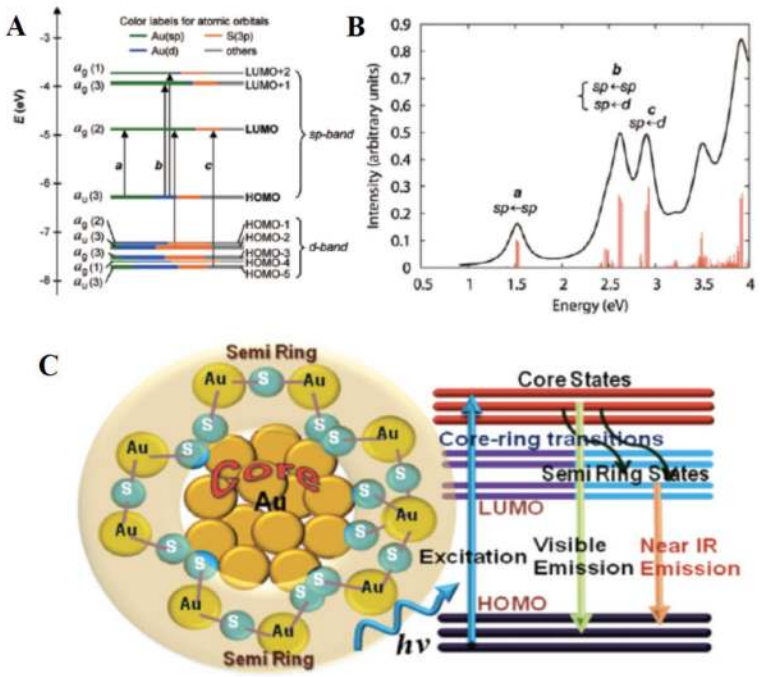

Figure 2.

(A) Kohn-Sham orbital energy level diagram for a model compound $Au_{25}(SH)_{18}^{-}$. (B) The theoretical absorption spectrum of $Au_{25}(SH)_{18}^{-}$. Peak assignments: peak ***a*** corresponds to 1.8 eV observed, peak ***b*** corresponds to 2.75 eV (observed), and peak ***c*** corresponds to 3.1 eV (observed). (C) Cartoon diagrams showing the relaxation pathways in $Au_{25}L_{18}$ clusters, where electrons in the ground states are excited to excited states of Au_{13} core and then either directly relax back to HOMOs of the core, emit at 500 nm or decay to the semiring states, followed by relaxing back to the ground states and emitting NIR photons. (Reprinted from Ref. 52 and 53, with permission from American Chemical Society.)

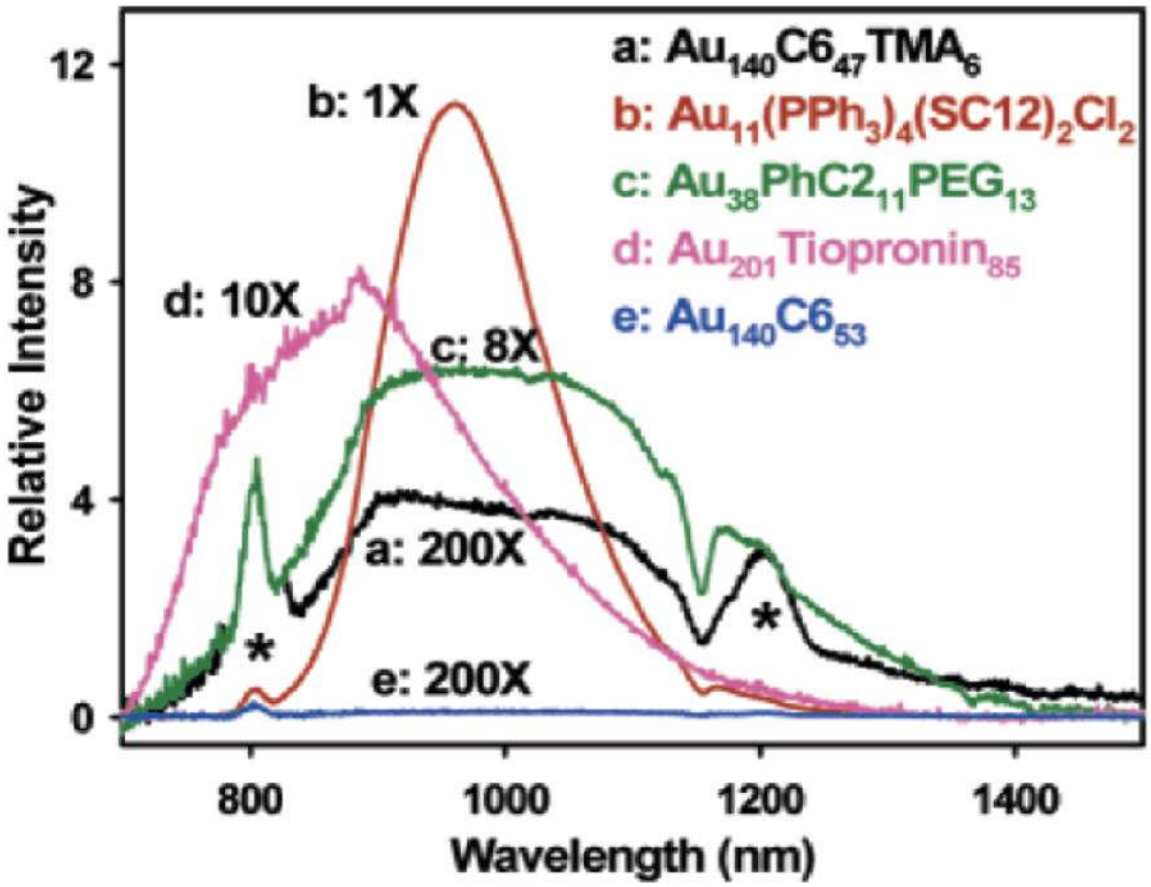

Figure 3.
IR emitting few-nm luminescent AuNPs with different core sizes and surface ligands. C6, C12, PhC2, PEG, and PPh3 represent hexanethiolate, dodecanethiolate, phenylethanethiol, poly(ethylene glycol) (MW 350) thiolate, and triphenylphosphine, respectively. (Reprinted from Ref. 34, with permission from American Chemical Society.)

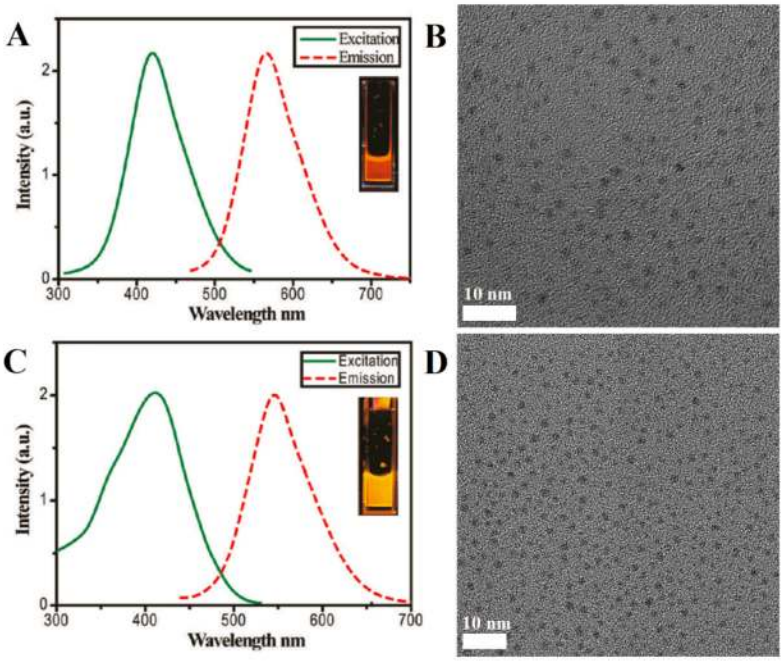

Figure 4.

Characterization of glutathione coated luminescent AuNPs. (A) The excitation and emission spectra of OGS-AuNPs in aqueous solution. Inset: Pictures of OGS-AuNPs taken with excitation of a hand-held long-wave UV lamp (365 nm). (B) Typical TEM image of OGS-AuNPs (scale bar: 10 nm). (C) The excitation and emission spectra of YGS-AuNPs in aqueous solution. Inset: Pictures of YGS-AuNPs taken with excitation of a hand-held long-wave UV lamp (365 nm). (B) Representative TEM image of YGS-AuNPs (scale bar: 10 nm). (Reprinted from Ref. 59, with permission from American Chemical Society.)

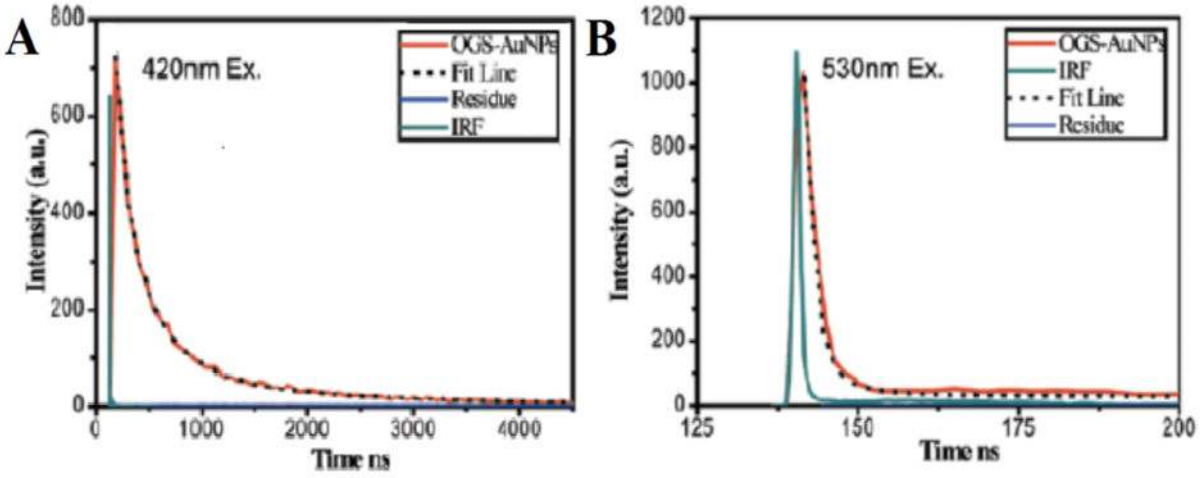

Figure 5.

Luminescent lifetimes of OGS-AuNPs. (A) The lifetime of OGS-AuNPs excited at 420 nm showing 1.7 μs (79%)/0.35 μs (21%). (c) The lifetime of OGS-AuNPs excited at 530 nm showing 2.8 ns (81%)/33 ns (19%). (Reprinted from Ref. 59, with permission from American Chemical Society.)

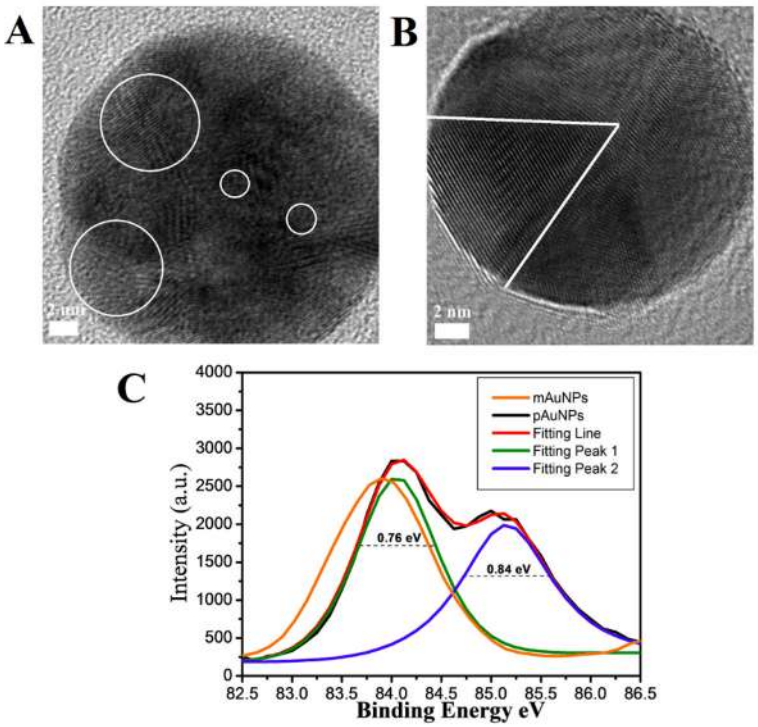

Figure 6.

Polycrystalline gold nanoparticles (pAuNPs) created in glycine matrices through a solid-phase thermal reduction method. (A) HR-TEM image of pAuNPs, containing many grains with size down to 1 nm (scale bar: 2 nm). Two 5 nm and two 1 nm representative individual grains are labeled with white circles. (B) Commercially available multi-twinned gold NP (mAuNP) composed of 8 nm grains (scale bar: 2 nm). (C) X-ray photoelectron spectroscopic measurements on Au $4f_{7/2}$ binding energy (BE) of pAuNPs and mAuNPs. Two peaks with maxima at 84.0 eV and 85.1 eV were observed from ~20 nm pAuNPs while only one peak at 83.9 eV was observed from the same size mAuNPs. (Reprinted from Ref. 81, with permission from Royal Society of Chemistry)

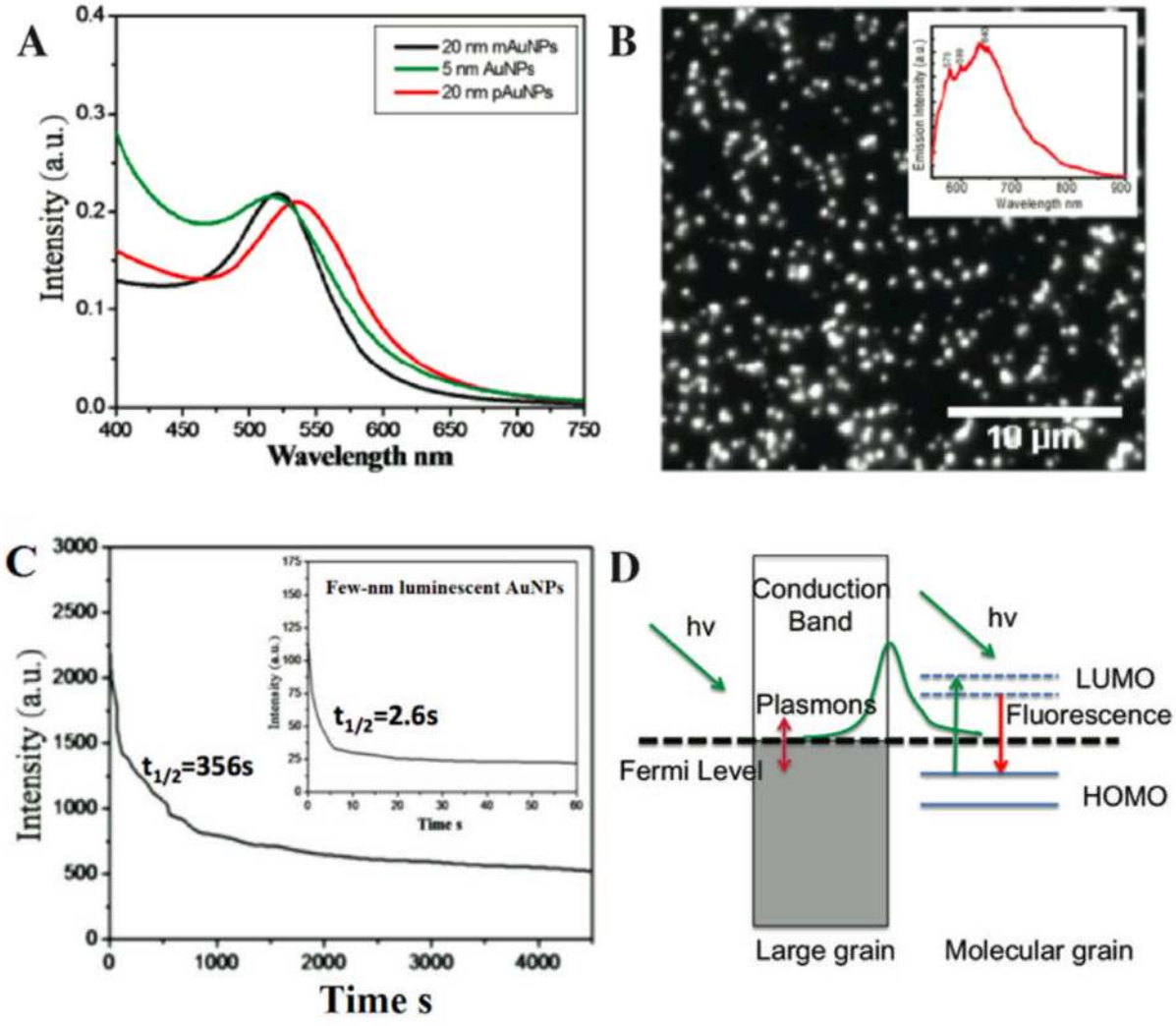

Figure 7.

Photophysical properties of pAuNPs. (A) UV-Vis absorption spectra of as-synthesized 20 nm pAuNPs, 20 and 5 nm mAuNPs aqueous solutions. The surface plasmon maximum of pAuNPs is located at 536 nm, which is red shifted about 16 nm compared to those of 5 and 20 nm mAuNPs. (B) Fluorescence image of individual pAuNPs. Inset: emission spectrum of pAuNPs under 532 nm laser excitation. (C) Photostability comparison of pAuNPs and few-nm luminescent AuNPs. (D) Hypothesized electronic structure and optical transitions in pAuNPs, where continuous electron band and discrete energy states co-exist within one single particle but are separated by energy barriers caused by grain boundaries and defects. (Reprinted from Ref. 81, with permission from Royal Society of Chemistry)

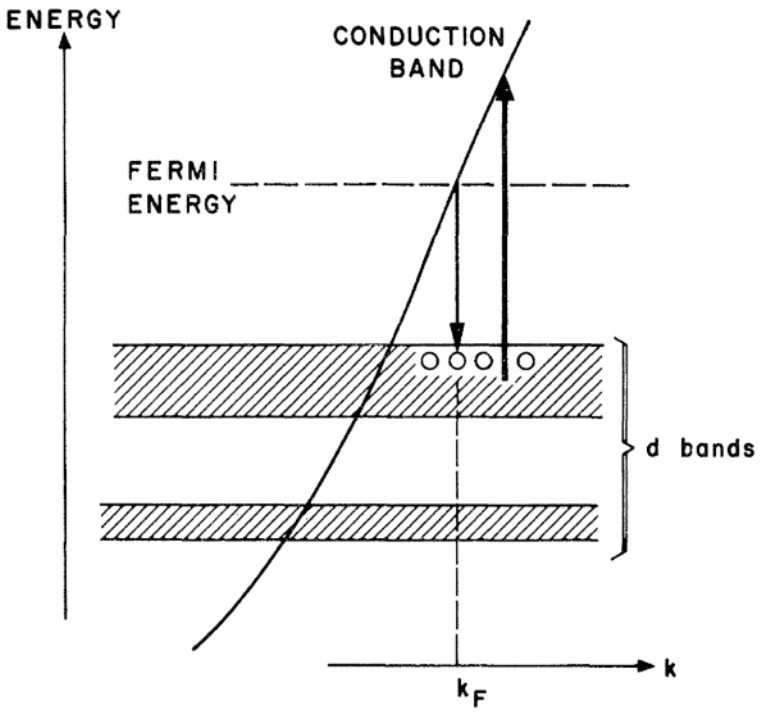

Scheme 1.
Schematic band structure of a noble metal showing the excitation and recombination transitions. (Reprinted from Ref. 15, with permission from American Physical Society)

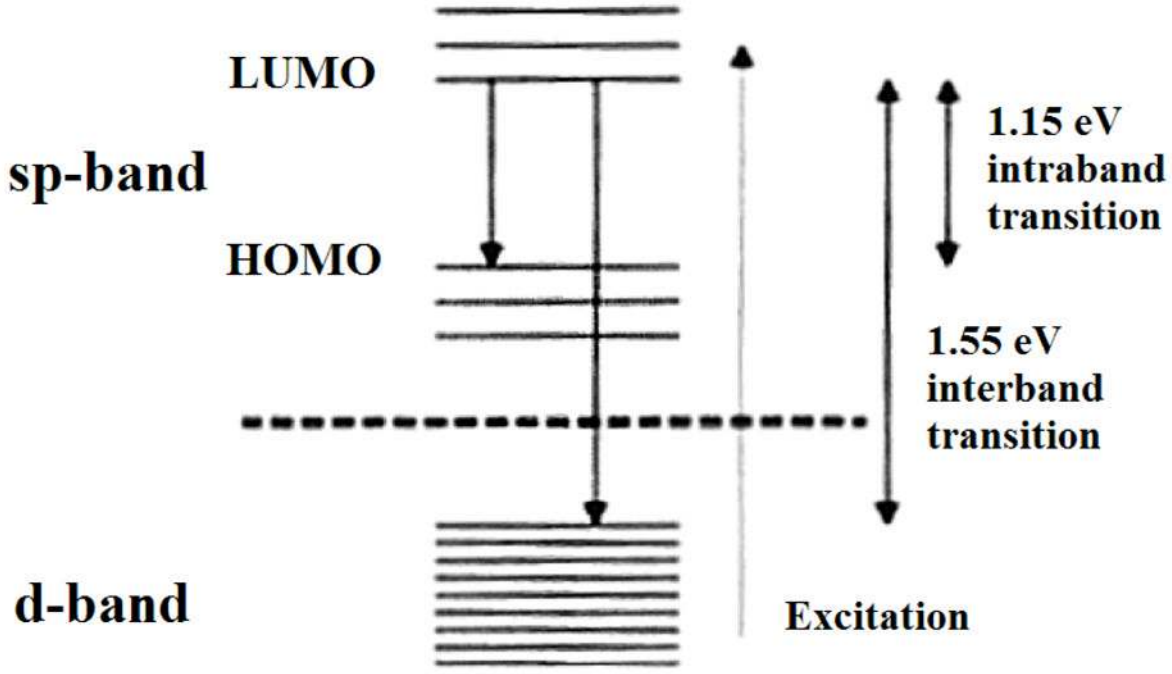

Scheme 2.

Solid-state model for the origin of the two luminescence bands from Au_{28} clusters. The high energy band is proposed to be due to radiative interband recombination between the sp and d-bands while the low energy band is thought to originate from radiative intraband transitions within the sp-band across the HOMO-LUMO gap. Note that intraband recombination has to involve prior nonradiative recombination of the hole in the d-band created after excitation with an (unexcited) electron in the sp-band. (Reprinted from Ref. 21, with permission from American Chemical Society.)

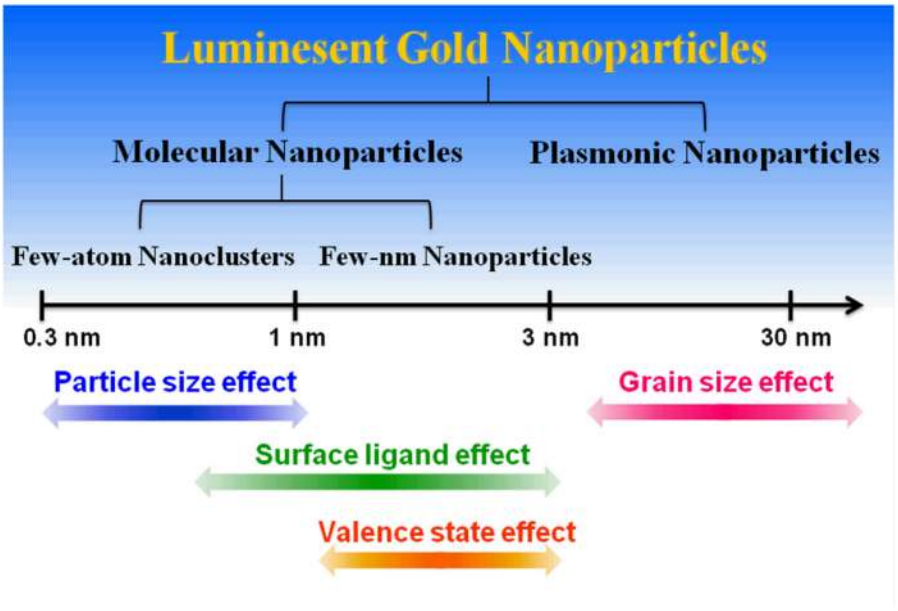

Scheme 3.

Luminescent AuNPs can be divided into two major classes: molecular NPs and plasmonic NPs. For molecular NPs, they can be further divided into two subclasses: Few-atom nanoclusters and few-nm NPs, where particle size, surface ligands and valence states all have significant impacts on the luminescence properties. For plasmonic NPs, grain size plays a key role in the emission.

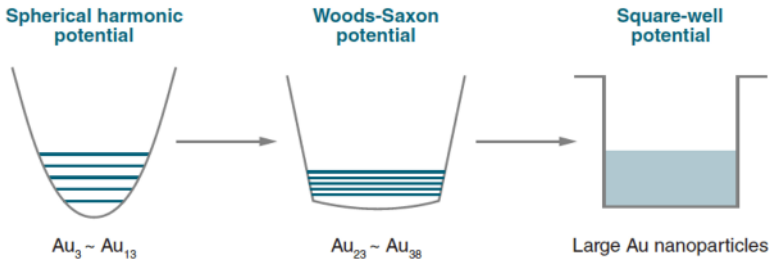

Scheme 4.

Schematic of size-dependent surface potentials of Au clusters on different size scales. For the smallest Au clusters (Au_3 to Au_{13}), cluster-emission energies can be well fit with the energy-scaling law $E_{Fermi}/N^{1/3}$, where N is the number of atoms in each cluster, indicating that electronic structure transitions of these small Au clusters are well-described by a spherical harmonic potential. With increasing size, small aharmonicities distort the potential well, which at larger sizes gradually distorts into a Woods-Saxon potential surface, and eventually becomes a square-well potential, characteristic of electrons in large metal NPs. (Reprinted from Ref. 36, with permission from American Physical Society.)

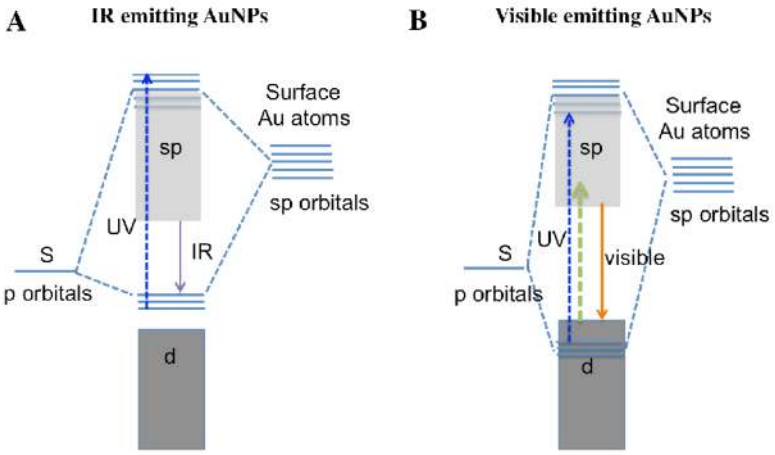

Scheme 5.

Hypothesized schemes for emission from IR and visible emitting luminescent few-nm AuNPs. In both cases, thiolated ligands form hybrid electronic states with surface gold atoms. However, valence states of surface Au atoms have significant influences on the emission wavelengths and lifetimes. (A) In IR emitting AuNPs, Au(0)-S hybrid electronic states (HOMO) formed through are between d and sp bands. (B) However, in visible emitting GS-AuNPs, the hybrid states are below some states in d band; as a result, emission fundamentally arises from sp to d band transitions.